Characterization of Layered GaSe Crystals Intercalated with $RbNO_3$ Ferroelectric Salt and their Application for Electric Capacitors

YuriyZhirko[1], VasiliyGrekhov[2], ZakharKovalyuk[3], Victor Netyaga[4]

[1,2]Institute of Physics, ProspektNauki, 46, 03028, Kiev, Ukraine
[3,4]Chernivtsy Branch of Institute for Material Science Problem, Vilde str., 5, 58001, Chernivtsy, Ukraine

Abstract— *XRD, SEM, EDX investigations as well as wide temperature (T = 5–300 K) photoluminescence measurements of GaSe single crystals intercalated from the melt of $RbNO_3$ ferroelectric salt at various temperatures and exposure times are performed in this work. Intercalation by this method results in GaSe matrix fragmentation by separate polycrystals 1 mm in size which consist of bulk GaSe segments (with sizes up to 50.0 mkm) and veins of $RbNO_3$ ferroelectric salt with thickness reaching 2–3 mkm. Within the GaSe segments are inclusions of nano-sized phases consisting of $RbNO_3$ salt whose diameter does not exceed 120 nm. It has been shown that the creation of GaSe<$RbNO_3$> hybrid structure has an insignificant influence on the optical properties of GaSe matrix, since in the photoluminescence spectra of GaSe<$RbNO_3$> at T = 300 K one can observe emission of free excitons which is typical for GaSe single crystals. The electrical investigations performed indicate that the intercalated GaSe<$RbNO_3$> or GaSe<KNO_3> are capable of accumulating electric energy, and prototypes of supercapacitors based on them possess: specific long-time energy 105 kJ/kg and resource of cycles > 10^6.*

Keywords— Layered crystal, GaSe, intercalation, ferroelectric, supercapacitors.

I. INTRODUCTION

Anisotropy of chemical bonds in layered crystals, weak van der Waals bonds between crystalline layers, and strong covalent bonds between adjacent atoms inside the layers define anisotropy of electric and dielectric properties of these crystals, which results in instability of synthesis when forming the crystalline lattice of these compounds. The following intercalation of the interlayer space in these crystals with foreign atoms or molecules, beside obtaining some expected changes in physical-and-chemical properties of hybrid materials based on them, finds its practical applications in power engineering, in particular, as solid-state hydrogen storages [1, 2], accumulators of electric energy [3], and sensors of physical fields [4]; moreover, heterostructures with high photosensitivity based on these materials can be applied in solar cells [5–7].

In this paper we present our recent investigation of some physical and chemical properties of GaSe single crystals intercalated in melts of $RbNO_3$ ferroelectric salt and done some estimates of their application as working materials for solid state supercapacitors in the up-to-date semiconductor element base.

II. EXPERIMENTAL METHODS

Pure GaSe crystals were grown using the Bridgman method from a stoichiometric melt. The obtained semiconductor layered single crystals had the following properties: hexagonal structure of ε-modification (space group D^1_{3h}) with unit cell parameters of a = 3.7549 ± 0.0002 Å, c = 15.9483 ± 0.0001 Å; conduction of p-type; carriers concentration of $2.3\cdot10^{15}$ cm^{-3}; and resistivity of $2.1\cdot10^9 \Omega\cdot cm$.

Then, from large ingots of the obtained single crystals, using mechanical spalling, we separated plates with sizes of 3 mm × 3 mm × 1 mm along the cleavage plane. In what follows, these plates were intercalated in the melt of $RbNO_3$ ferroelectric salt.

Intercalation in the melt was realized in the following manner. Ferroelectric material of rubidium nitrate was melted in a porcelain crucible (chemically inert in the melt) at a temperature within the range of 365–411 ºC. The melting temperature of $RbNO_3$ is 313.3 °C. The temperature of melt was automatically maintained by a temperature regulator with accuracy ± 0.1 ^{0}C. The samples of GaSe single crystals were wholly dipped into the melt, where the process of $RbNO_3$ intercalation into the layered crystal GaSe took place. The principal setup of the facility for intercalation in the melt is shown in Fig. 1. The process of intercalation and "*in-situ*" measurements was performed in a hermetic box in air dried with P_2O_5.

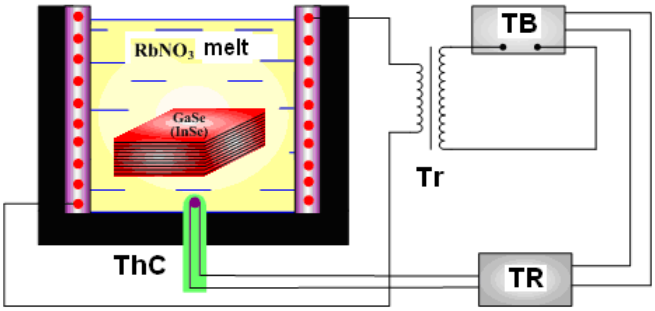

FIG. 1 SCHEME OF GaSe INTERCALATION IN $RbNO_3$ MELT. HERE: Tr – TRANSFORMER, TB – THYRISTOR BLOCK, TR – TEMPERATURE REGULATOR, ThC – THERMOCOUPLE

Fig. 2 shows stereo-microscopic images (Leika) of the cleavage surfaces of GaSe crystals intercalated in the $RbNO_3$ melt at various temperatures and times of exposure. As can be seen, intercalation in the melt results in fragmentation of the crystalline matrix.

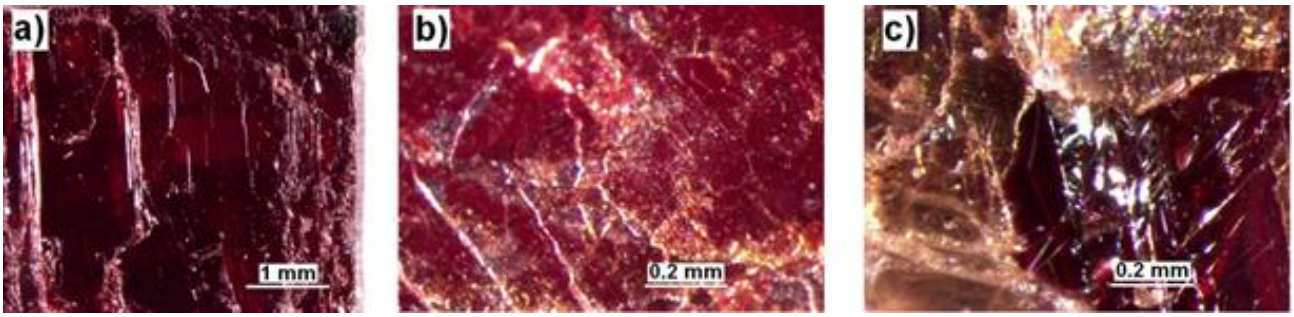

FIG. 2. STEREO-MICROSCOPIC IMAGES OF CLEAVAGE SURFACES OF THE INTERCALATE GaSe<$RbNO_3$> AFTER EXPOSURE OF THE GaSe CRYSTAL IN THE MELT OF $RbNO_3$ SALT FOR VARIOUS TIME AT A TEMPERATURE OF 367 °C: a) sample #1 - 17 min, b) sample #2 - 32 min, c) sample #4 - 68 min.

In addition to fragmentation of the GaSe crystal, in the process of its intercalation in the $RbNO_3$ melt, growth of the mass and thickness of the sample is observed. As seen in Fig. 3, in the first stage, one can observe a noticeable increase in the mass and thickness of the sample. In the second stage, this growth is insignificant, but in the third stage the mass and thickness of the sample grow very fast, accompanied by subsequent destruction of GaSe< $RbNO_3$>intercalate. This part of the experiment is described in more detail in [8].

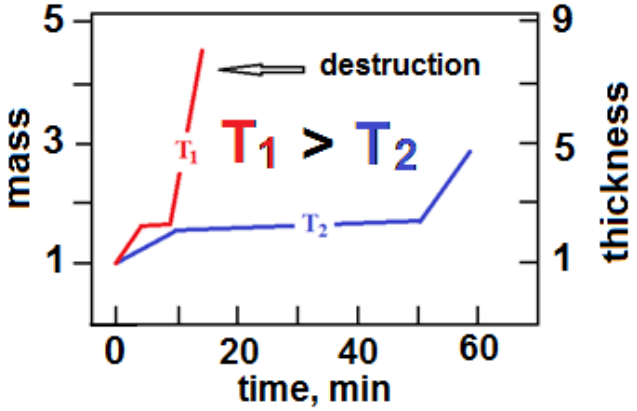

FIG. 3. DEPENDENCES OF THE MASS AND THICKNESS OF GaSe<$RbNO_3$>INTERCALATE ON THE TIME AND TEMPERATURE OF THE $RbNO_3$ MELT.

2.1 Electron-microscopic and energy-dispersion investigations of GaSe<$RbNO_3$> intercalates

Characterization of GaSe crystals and GaSe<RbNO3> intercalates was done ne scanning electron microscope (SEM, Vega3 SBU, Tescan) equipped with secondary-electron (SE) and back-scattering electron (BSE) emission detectors as well as EDX spectrometer (Oxford Instruments) with an X-act (10 mm^2) SSD detector and Inca EDS Software.

Fig. 4 shows the technological (external) surface of GaSe single crystal intercalated in the $RbNO_3$ melt. After intercalation, this surface has new formations in the form of dendrites of various shapes and sizes. It is noteworthy that these new formations define the mass and thickness of intercalated samples to some extent. At the same time, the spot in Fig. 4a indicates the part of the crystal that was investigated using the energy-dispersion analysis of the chemical composition of this technological surface.

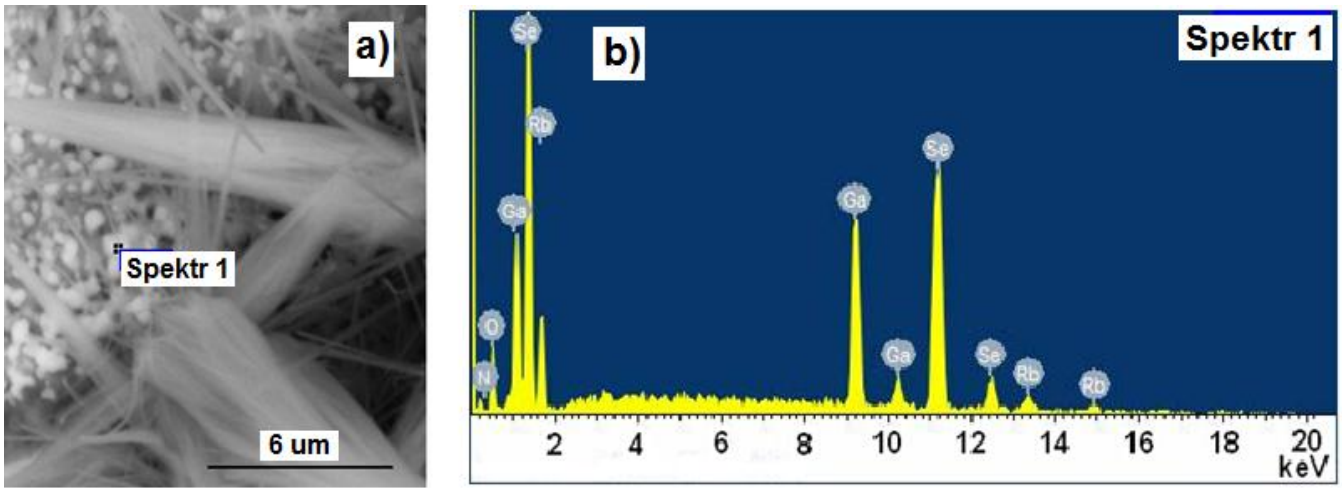

FIG. 4. A) ELECTRON-MICROSCOPIC IMAGE OF TECHNOLOGICAL SURFACE OF GaSe<RbNO3>; b) EDX SPECTRA OF SELECTED POINT ON TECHNOLOGICAL SURFACE OF GaSe<$RbNO_3$> INTERCALATE

Fig. 4b shows the EDX spectrum of the spot illustrated in Fig. 4a. In this spectrum, one can see the peaks corresponding both to the Ga and Se atoms that form the matrix and to the Rb, N, and O atoms related with the ferroelectric salt. The concentration of atoms at the technological surface differs to some extent from the stoichiometric compositions of the GaSe matrix and $RbNO_3$ salt.

Fig. 5 shows the cleavage surface of GaSe<$RbNO_3$> intercalate for various magnifications in the range of 251× to 50,000×. Juxtaposing Figs. 2 and 5, one can see that after intercalation in the $RbNO_3$ melt, the monocrystalline GaSe matrix forms disordered crystalline blocks (up to 1 mm in size), that is, it becomes polycrystalline. Inside large blocks, one can observe further segmentation of the matrix with the creation of $RbNO_3$ salt veins between the segments.

In our opinion, these veins are created during intercalation in the places of dislocations and point defects in GaSe, which results in the appearance of stress-strain regions in the lattice of polycrystals. The above veins of $RbNO_3$ salt possess complex 3D forms, and their thickness reaches 2 to 3 mkm. Also, one can see that inside the segments, whose sizes reach 50 mkm (Figs. 5c to 5d), there are inclusions of the ferroelectric salt solid phase that are non-uniformly distributed inside the segments. The mean diameter of these inclusions does not exceed 120 nm.

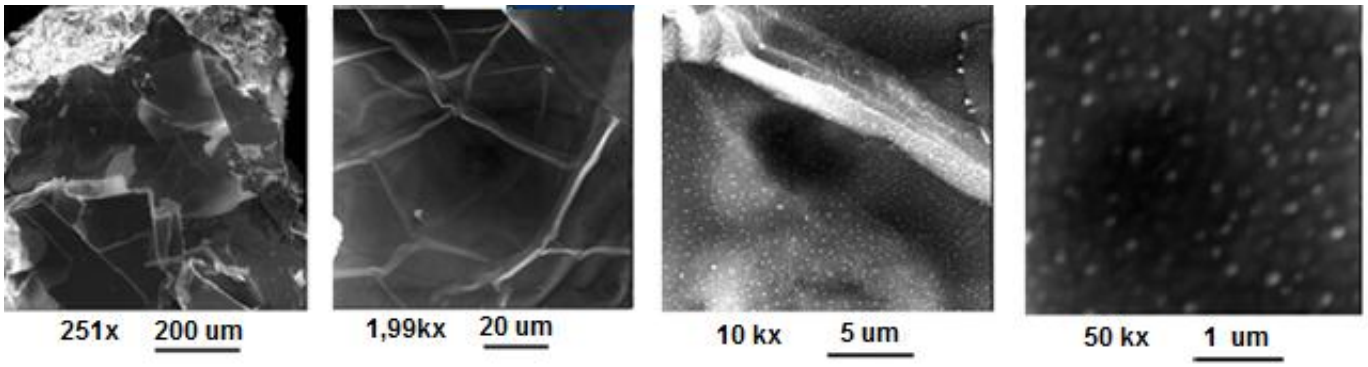

FIG. 5. SEM IMAGES OF THE FRESH CLEAVAGE SURFACE OF THE GaSe<$RbNO_3$> INTERCALATE AT MAGNIFICATIONS OF 251× to 50,000×.

As can be seen from Figs. 5c and 5d, the concentration of $RbNO_3$ inclusions related to the total scanned surface in the SEM image rages from 2 to 10% in segments of the GaSe matrix and up to 100% in the $RbNO_3$ veins.

2.2 X-ray diffraction investigations

Fig. 6 presents the XRD spectrum of GaSe<$RbNO_3$> intercalates obtained using the diffractometer DRON-3. As seen in this spectrum, beside the diffraction peaks corresponding to the GaSe crystal, there are peaks corresponding to the crystals of $RbNO_3$ salt.

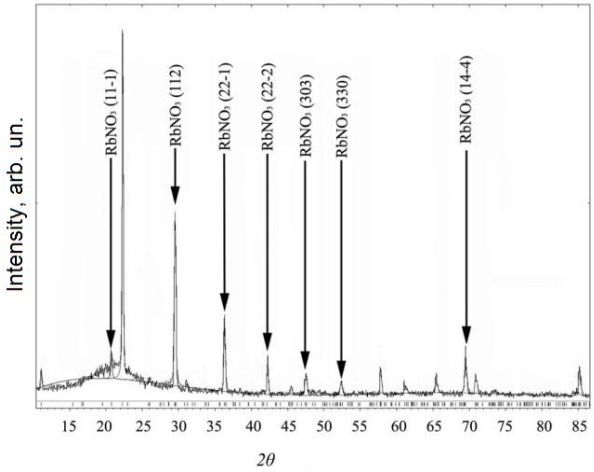

FIG. 6.DIFFRACTOGRAM OF THE COMPOSITE NANOSTRUCTURE GaSe<$RbNO_3$>. THE ARROWS INDICATE DIFFRACTION PEAKS INHERENT TO THE $RbNO_3$ CRYSTALLINE PHASE.

The obtained XRD data confirms that the intercalation process in the GaSe single crystal leads to the transition of the unit cell belonging to GaSe in ε-modification to that observed in δ-modification, whose parameters are as follows: a = 3.7550 Å and c = 31.8903 Å. In accordance with [9], the unit cell in δ-modification consists of four crystalline layers. When intercalating the GaSe matrix from the melt, the parameter a is practically unchanged, while the parameter c is noticeably reduced. This reduction of c parameter is caused by pressure that is related to the embedding of the $RbNO_3$ inclusions into the GaSe matrix. Indeed, according to [10], the hydrostatic pressure in GaSe crystals reduce the width of van der Waals gap and the length of double bond between Ga atoms inside the GaSe crystalline layer and also reduce the parameter c, while the parameter a remains unchanged.

In the case of the $RbNO_3$ ferroelectric salt intercalated to the GaSe crystal, the growth of both parameters in the $RbNO_3$ unit cell (a = 10.4996 Å and c = 7.3810 Å) is involved. It should be noted that standard parameters of the $RbNO_3$ salt unit cell in our investigations were a = 10.4352 Å and c = 7.3710 Å, in full agreement with the literature data [11].

These changes in the parameters of the GaSe and $RbNO_3$ unit cells indicate creation of mechanical stress-strain states at the boundaries between the matrix and intercalant, which causes pressure inside the GaSe< $RbNO_3$> intercalate. In turn, it results in rupture (crushing) of crystalline layers and segmentation of the GaSe matrix.

Using the crystals InSe and GaSe as examples, earlier XRD investigations showed that electrochemical intercalation of these layered crystals with hydrogen [1] results in growth of the parameter c due to increasing of the width of van der Waals gap in the crystal. At the same time, SEM investigations confirmed that intercalation of GaSe and InSe crystals in solutions of hydrogen-containing molecules (H_2O, C_2H_5OH, C_6H_7) leads to swelling of the van der Waals gap [2]. However, in both of these cases of intercalation with hydrogen or hydrogen-containing molecules, segmentation of GaSe and InSe matrixes was not observed even after cooling them down to T = 5 K and then heating them up to room temperature.

Also, it was shown in [1, 2] that hydrogen and hydrogen-containing molecules are intercalated and de-intercalated from these layered crystals without any destruction of the crystal, and the concentration of hydrogen molecules during intercalation reaches 2 to 3 per molecule of Ga_2Se_2.

This different reaction of the matrix from the reaction of the chemical compound intercalated in it can be related to the difference in the physico-chemical properties of the hydrogen-containing molecules and ferroelectric salts in the matrix of GaSe (InSe). In accordance with [1, 2], the hydrogen-containing molecules passivate point defects (donors/acceptors) of the layered GaSe (InSe) matrix. On the contrary, $RbNO_3$ pass its Rb or O atoms to point and spatial defects of GaSe matrix which create different intermediate chemical compounds between them. The thickness of these intermediate compounds can vary between one and several molecules of GaSe and $RbNO_3$.

Juxtaposing between: i) optical images of cleavage surfaces for the GaSe<$RbNO_3$> intercalates, dependences of the mass and thickness of samples on the time of their intercalation in the melt of ferroelectric salt at various temperatures, data obtained from SEM, EDX, and XRD investigations of the GaSe<$RbNO_3$> intercalates; and ii) taking into account the classical theory of materials strength (and considering in this model action of the $RbNO_3$ salt intercalated into GaSe as an external pressure applied to the GaSe monocrystalline matrix) one can make the following assumption:

- Three stages of growth of the thickness and mass of the samples with time and temperature of intercalation of the layered GaSe matrix with the $RbNO_3$ salt are similar to the three stages of application of the external force that stretches or compresses the studied solid.

Namely,

- in the first stage, the process of intercalating the GaSe matrix with the $RbNO_3$ melt corresponds to the Hooke law (nano-formations of the $RbNO_3$ salt are created in GaSe matrix);
- in the second stage, plastic deformation of the GaSe matrix takes place, with a possible transition from one modification to another;
- The third stage corresponds to fragmentation of the GaSe matrix, which is completed by its destruction.

Also, it is worth noting that ferroelectrics possess the so-called "soft modes", which lead to phase transitions in ferroelectrics under the changes in temperature. This should also be taken into account when cooling the GaSe<$RbNO_3$> intercalate down to the room temperature after extraction from the $RbNO_3$ melt.

2.3 Photoluminescence spectra

Measurements of photoluminescence (PL) spectra were made using a 0.6-m optical spectrometer MDR-23 (LOMO) with a grating 1200 grooves/mm. Investigations of PL spectra at T = 5–300 K were made using a helium cryostat A-255 designed at the Institute of Physics NAS of Ukraine. It was equipped with a UTRECS K-43 system allowing control of a sample temperature within the range 4.2 to 330 K with an accuracy of 0.1 K.

The excitation of PL spectra was performed using a current-wave semiconductor laser with a wavelength of 532 mn and stable power at 100 mW equipped with laser (SL-532-10 Thorlabs) and edge (LP-03-532-RS Semrocks) filters. An a FEU-79 photomultiplier tube was served as the radiation detector. The slit spectral width of monochromator did not exceed 0.2 meV at T = 5 K and 0.5 meV at T = 300 K.

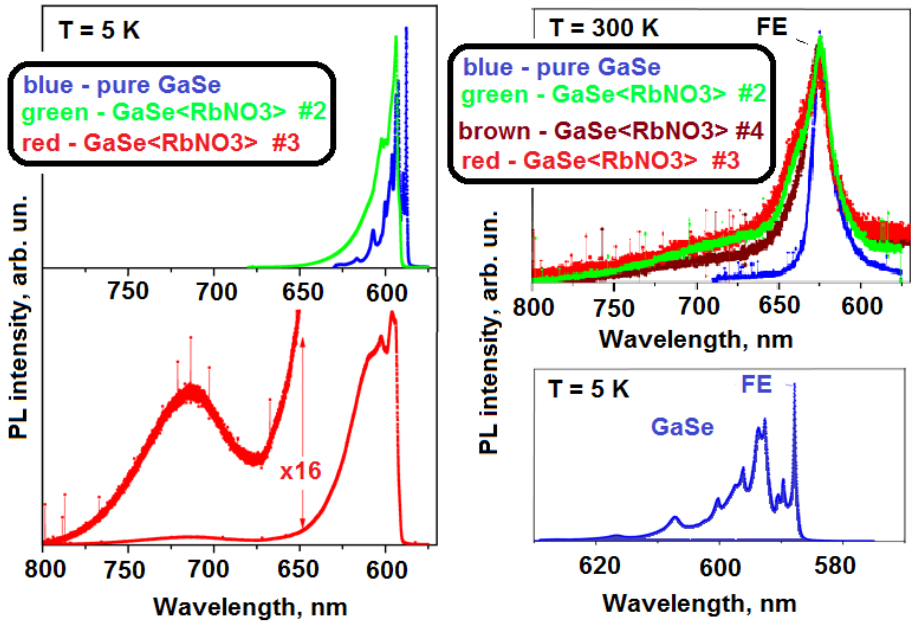

FIG. 7. PHOTOLUMINESCENCE SPECTRA: (A) AND (B) FOR THE GaSe SINGLE CRYSTALS AND SAMPLES #2 AND #3 OF THE GaSe<$RbNO_3$> INTERCALATES AT T = 5 K; (C) FOR THE GaSe CRYSTAL AND THE SAMPLES #2, #3 AND #4 OF THE GaSe<$RbNO_3$> INTERCALATES AT T = 300 K; (D) FOR THE GaSe SINGLE CRYSTAL T = 5 K. THE TEMPERATURE OF GaSe<$RbNO_3$> MELT WAS 367 °C

Fig. 7 are the photoluminescence spectra at the temperatures of $T = 5$ and 300 K for GaSe single crystals and the samples of GaSe<$RbNO_3$> intercalates prepared under various exposure times and the melt temperature of 367 °C.

As it can be seen in Fig. 7d, at $T = 5$ K the PL spectrum of GaSe crystal consists of lines corresponding to radiation of the free excitons (ƛ = 587.8 nm, $E_{exc} = 2.108$ eV) [12] as well as of excitons bound to stacking faults of crystalline layers, dislocation, and point defects. Besides, the PL spectrum in the range $E < 2.050$ eV (ƛ> 605.0 nm) contains several bands of a low intensity which, according to [4], are caused by transitions between the direct and indirect conduction bands and shallow acceptors in GaSe<$RbNO_3$>.

As seen in Fig. 7a, the PL spectra of the GaSe<$RbNO_3$> intercalates do not contain emission lines of free excitons or excitons localized at the stacking faults of crystalline layers [13–15] or at extended spatial defects of the dislocation type. But emission lines of excitons localized on point defects (see sample #3) and broad band's associated with radiative recombination of electrons from direct/indirect conduction bands at the deep acceptor levels (155, 190, 310, and 460 meV) with participation of one to three optical fully symmetric (A) or polar (LO, TO) phonons of crystalline lattice are available in these spectra. The similar optical transitions in the forbidden gap depth are also observed in GaSe crystals doped with 3-d elements of the iron group at concentrations up to 1 wt. %, and take place between direct/indirect conduction bands and deep acceptor levels with participation of optical phonons [4].

The results of these investigations clearly indicate imperfection of the GaSe crystal, which is caused by its intercalation in the melt of $RbNO_3$ salt. This imperfection defines lowering the polariton lifetime in the exciton-like state, fast exciton localization, and recombination near defects. Therefore, at $T = 5$ K one cannot observe emission of free excitons in the GaSe<$RbNO_3$> intercalates.

Growth of the temperature up to 300 K in the GaSe single crystal sample leads to uniform scattering of free exciton by phonons of the crystalline lattice [16]. As a consequence, the lifetime of polariton in the exciton-like state becomes lower than the time of exciton localization on the defect. Therefore, in the PL spectrum of GaSe single crystal (Fig. 7c) only the emission line of free excitons remains at T = 300 K.

In the case of GaSe<$RbNO_3$> at $T = 300$ K, like the case of GaSe single crystals, one can observe emission of free excitons, which is accompanied by emission of broad bands caused by radiative recombination of electrons from direct/indirect conduction bands to the deep acceptor levels (155 and 190 meV) with participation of one to three optical full-symmetric or polar phonons of the crystalline lattice.

Up to the experimental accuracy, one can state that the energy of the emission line corresponding to free exciton in the GaSe crystal and in GaSe<$RbNO_3$> intercalates coincides. It is indicative of the fact that under intercalation from the melt, the width of the forbidden gap in GaSe polycrystalline blocks (which is defined by electron orbitals of adjacent atoms Ga and Se in the crystalline layer) does not change even in the presence of $RbNO_3$ salt nano-formations in the matrix. Therefore, one can state that lowering of the parameter c in the GaSe polycrystalline matrix intercalated with $RbNO_3$ salt takes place due to lowering the width of the van der Waals gap.

Taking into account the size of GaSe matrix segments in the GaSe<$RbNO_3$> intercalates, the so-called "blue shift" of free excitons can be neglected.

Thus, one can draw a conclusion that the GaSe<$RbNO_3$> polycrystalline matrix keeps the optical properties inherent in monocrystalline GaSe, despite the fact that, during intercalation from the ferroelectric salt melt, large spatial veins and nanoparticles of $RbNO_3$ are embedded there.

2.4 Development of supercapacitor prototype and studying of its properties

The prototype of a supercapacitor based on the GaSe<$RbNO_3$> or GaSe<KNO_3> intercalates whose electric and dielectric properties were investigated was developed in the following way. We deposited plain conducting ohmic contacts with leads onto the planes of intercalated samples GaSe<$RbNO_3$> or GaSe<KNO_3> (oriented along the normal to the crystallographic axis C) which were spalled from both sides of the surfaces. Then, the sample as a whole was sealed with a silicon sealant. The prototype prepared in this way was investigated as an accumulator of electric energy. The basic sketch of the supercapacitor based on the GaSe<$RbNO_3$> intercalate is shown in Fig. 8a; and a photograph of this prototype covered with a metal envelope is presented in Fig. 8b.

We applied the constant electric field with the voltage 200 V to the contacts of the prototype shown in Fig. 8 for 10 min. As a result, after stopping the action of the external electric field, the capacitor plates kept the voltage close to 19.5 V. The specific long-time energy was higher than 105 kJ/kg. The specific energy was 29.1 W·h/kg

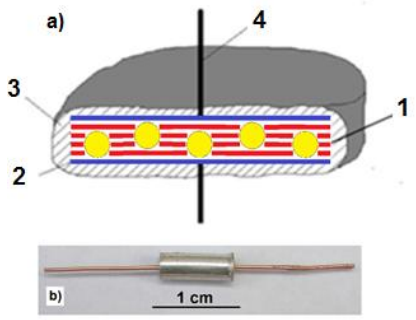

FIG. 8 A) BASIC SKETCH OF THE SUPERCAPACITOR PROTOTYPE. HERE: 1 – GaSe<KNO_3> or GaSe<$RbNO_3$> INTERCALATE (YELLOW BALLS – $RbNO_3$ SALT); 2 – CURRENT-CONDUCTING PLANE CONTACT (BLUE); 3 – COMPOUND ENVELOPE; 4 – CURRENT TAP. B) PHOTOGRAPH OF THE SUPERCAPACITOR PROTOTYPE.

The studied capacitor of electric energy capable of operating within the range of 50 to 200 V; its operation temperature lies within the interval of –40 to +50 °C; and its number of charge cycles > 10^6.

Table 1 summarized the data comparing the energy performances of the proposed electricfl energy capacitor based on the GaSe<KNO_3> intercalate and other supercapacitors.

TABLE 1
SOME TECHNICAL PERFORMANCES OF THE OFFERED GaSe<KNO_3> PROTOTYPE AND OTHER SUPERCAPACITORS

	C, F	$C_{spesific}$, F/g	$C_{specific}$, F/cm3
Maxwell	3000	6	68
Loxus	5000	12,5	110
Wima	5000	1,76	1,8
Nesscap	5000	11,11	100
Prototype GaSe<KNO3>	58	2148	2320

III. CONCLUSIONS

From the performed investigations of processes taking place in GaSe crystals when intercalating them in the melt of ferroelectric salt $RbNO_3$ and studying the physical and chemical properties of the prepared GaSe<$RbNO_3$> intercalates, the following features could be ascertained:

1. Non-monotonous growth of the mass and thickness of the crystal takes place over time. This process consists of three stages: i) the mass and thickness of the sample grow; ii) the mass and thickness of the sample are not practically changed with time; iii) both parameters increase to the limit when matrix destruction is observed.

In accord with the classical theory of the strength of materials, intercalation of the GaSe matrix in the first stage obeys Hooke's law: nanoparticles of $RbNO_3$ salt are formed in this matrix, resulting in growth of the mass and thickness of the sample. In the second stage, plastic deformation of the GaSe matrix takes place with a possible transition to another modification, when GaSe bulk polycrystals are created. In the third stage, we observe a transition to final fragmentation of the GaSe matrix when veins of $RbNO_3$ salt are created between these fragments. Further intercalation is completed by destruction of the GaSe matrix.

2. In the process of intercalation, the GaSe matrix becomes polycrystalline, and these polycrystals (with the sizes up to 1 mm) consist of segments (with sizes of up to 50 mkm), between which ferroelectric salt veins of a complex 3D form are created, whose thickness is close to 2 – 3 mkm. Inside the matrix segments, one can observe non-uniformly distributed inclusions of ferroelectric salt with a mean size of 120 nm. The concentration of these inclusions in the matrix segments reaches 2% to 10% and becomes 100% in the veins between segments.

3. The unit cell of the GaSe single crystal in ε-modification makes the transition into δ-modification, which consist of four crystalline layers with the following parameters: a = 3.7550 Å and c = 31.8903 Å. This lowering of the parameter c takes place due to a reduction in the width of the van der Waals gap caused by pressure related with embedding the veins and nano-sized $RbNO_3$ inclusions in the GaSe matrix.

4. Both parameters of the unit cell of the ferroelectric salt $RbNO_3$are increased to a = 10.4996 Å and c = 7.3810 Å.

5. Despite the creation of a large numbers of defects (veins and nanoparticles of $RbNO_3$) during intercalation by using the "from the melt" method, the GaSe polycrystalline matrix retains the optical properties inherent in the GaSe single crystal. At the same time, the number of point and spatial defects becomes larger, which creates deep acceptor levels responsible for the processes of radiative recombination of electrons from direct/indirect conduction bands with participation of one to several optical phonons.

6. The electrical investigations performed indicate that the intercalated GaSe<$RbNO_3$> or GaSe<KNO_3> can find application as working materials for solid state supercapacitors in the up-to-date semiconductor element base. They are capable of accumulating electric energy, and prototypes of supercapacitors based on them possess: specific long-time energy 105 kJ/kg and resource of cycles > 10^6.

ACKNOWLEDGEMENTS

Performing these investigations became possible owing to the project No. 0108U000252 within the framework of the departmental subject area in the National Academy of Sciences of Ukraine in accord with the Program for Scientific Instrument Engineering.

Also, the authors are very grateful to Dr. Z.R. Kudrynskyi for fruitful discussion of the experimental results obtained in this work.

REFERENCES

[1] Y.Zhirko, V.Trachevsky, and Z.Kovalyuk, "On the possibility of layered crystals application for solid state hydrogen storages – InSe and GaSe crystals", In book: "Hydrogen storage", by Editor Jianjun Liu, (ISBN) 978-953-51-0731-6, InTech, 2012, pp.211– 242.

[2] Y. Zhirko, V. Grekhov, N. Skubenko, Z. Kovalyuk,and T.Feshak, "Characterization and optical properties of layered InSe and GaSe crystals intercalated with hydrogen and oxygen-hydrogen-containing molecules", In book: "Advanced Materials for Renevable Hydrogen Production, Storage and Utilization",by Editor Jianjun Liu, (ISBN) 978-953-51-2219-7, InTech, 2015, pp.11–50.

[3] I.I. Grigorchak, A.V.Zaslonkin, Z.D. Kovalyuk et al., Patent of Ukraine (2002), Bulletin No5, No46137.

[4] Y.I. Zhirko, N.A. Skubenko, V.I. Dubinko, Z.D. Kovalyuk,and O.M. Sydor, "Influence of Impurity Doping and γ-Irradiation on the Optical Properties of Layered GaSe Crystals", Journal of Materials Science and Engineering B, pp.91–102, 2012.

[5] A.A. Lebedev, V.Yu. Rud', and Yu.V. Rud', "Photosensitivity of geterostructures porous silicon-layered $A^{III}B^{VI}$ semiconductors", Fiz.Tekch. Polupr. (in Russian),vol.32,pp.353–355, 1998.

[6] J. Martines-Pastor, A. Segura, and J. L. Valdes,"Electrical and photovoltaic properties of indium-tin-oxide/p-InSe/Au solar cells", J. Appl. Phys., vol. 62,pp.1477–1483, 1987.

[7] S. Shigetomi, and T. Ikari, "Electrical and photovoltaic properties of Cu-doped *p*-GaSe/*n*-InSe hetero-junction", J. Appl. Phys.,vol. 88 pp.1520–1524, 2000.

[8] Z.R. Kudrynskyi, and V.V. Netyaga, "Nanocomposite Material Based on GaSe and InSe Layered Crystals Intercalated by $RbNO_3$ Ferroelectric", Journal of Nano- and Electronic Physics, vol. 5,03028(7pp), 2013.

[9] A.Polian, K. Kunc, and A. Kuhn,"Low-frequency lattice vibrations of δ-GaSe compared to ε- and γ- polytypes", Sol. St. Commun., vol.19, pp.1079–1082, 1976.

[10] D.Olguin,A.Cantarero,C.Ulrich,and K.Suassen,"Effect of pressure on structural properties and energy band gaps of γ-InSe",PhysicaStatusSolidi (b), vol.235, pp.456–463,2003.

[11] V.E. Plustchev, andB.D. Stepin, "Chemistry and technology of lithium, rubidium, and cesium compounds",Moscow: Khymija, 1970.

[12] Yu.P. Gnatenko, P.A. Skubenko, Yu.I. Zhirko, and O.V.Fialkovskaya,"Emission of Free and Bound Excitons in GaSe and InSe Crystals in Direct and Indirect Transition Region", J. Luminescence,vol. 31&32, pp.472–475, 1984.

[13] N. Kuroda, and Y. Nishina,"Stacking-fault splitting of exciton spectrum in GaSe",NuovoCimento, vol.32B, pp. 109–115, 1976.

[14] Le Chi Thanh, and C. Depeursinge, "Fine structure of the exciton spectrum in GaSe", Sol. St. Com., vol.25, pp. 499–503, (1978).

[15] Y. Sasaki, and Y. Nishina, "Mobile and immobile localized excitons induced by the stacking faults in GaSe", Physica, vol. BC105, pp.45–49, 1981.

[16] Yu.I. Zhirko,"Investigation of the light absorption mechanisms near exciton resonance in layered crystals. Part 2. N=1 state exciton absorption in GaSe", PhysicaStatusSolidi (b), vol.219, pp.47–61, 2000.